

## Edge Currents as a Signature of Flatbands in Topological Superconductors

Andreas P. Schnyder,<sup>1,\*</sup> Carsten Timm,<sup>2,†</sup> and P. M. R. Brydon<sup>2,‡</sup>

<sup>1</sup>Max-Planck-Institut für Festkörperforschung, Heißenbergstrasse 1, D-70569 Stuttgart, Germany

<sup>2</sup>Institute of Theoretical Physics, Technische Universität Dresden, D-01062 Dresden, Germany

(Received 21 February 2013; published 13 August 2013)

We study nondegenerate flatbands at the surfaces of noncentrosymmetric topological superconductors by exact diagonalization of Bogoliubov–de Gennes Hamiltonians. We show that these states are strongly spin polarized and acquire a chiral dispersion when placed in contact with a ferromagnetic insulator. This chiral mode carries a large edge current which displays a singular dependence on the exchange-field strength. The contribution of other edge states to the current is comparably weak. We hence propose that the observation of the edge current can serve as a test of the presence of nondegenerate flatbands.

DOI: [10.1103/PhysRevLett.111.077001](https://doi.org/10.1103/PhysRevLett.111.077001)

PACS numbers: 74.50.+r, 74.20.Rp, 74.25.F–

*Introduction.*—The bulk gap of topological insulators and superconductors plays an essential role in defining the topological invariants and hence for the topological protection of their surface states [1–4]. Recently, however, the topological classification of matter has been extended to *gapless* systems, such as Dirac or Weyl semimetals [5,6] and nodal superconductors [7–10]. A bulk-boundary correspondence exists for certain surfaces, yielding topologically protected dispersionless zero-energy states, so-called “arc lines” or “flatbands.” Well-known examples are the zero-energy edge states of cuprate superconductors and the A phase of <sup>3</sup>He.

A promising materials class for topological systems is the noncentrosymmetric superconductors (NCSs), characterized by strong antisymmetric spin-orbit coupling (SOC) and a mixing of spin-singlet and spin-triplet pairing [11]. The superconducting gap in many of these compounds is reported to display line nodes, e.g., in CePt<sub>3</sub>Si [12,13], CeIrSi<sub>3</sub> [14], and Li<sub>2</sub>(Pd<sub>1-x</sub>Pt<sub>x</sub>)<sub>3</sub>B [15–17], and they can therefore support topological flatband surface states. Because of the exotic gap structure of NCSs, these flatbands are predicted to be *nondegenerate*, i.e., Majorana fermions [7,18–22], in contrast to the doubly degenerate flatbands found in other systems. Demonstrating that the surface flatbands of an NCS are nondegenerate presents a challenge, however: While typical experimental methods, such as tunneling conductance spectroscopy, are sensitive to the singular surface density of states contributed by the flatbands, they cannot probe the degeneracy.

In this Letter, we propose the response of the nondegenerate flatbands to a proximity-induced exchange field as an unambiguous test of their existence. We lay the foundation for our approach by demonstrating that the flatband states are strongly spin polarized, which in itself is an important experimental signature. The spin polarization originates from both the SOC and the spin structure of the superconducting gap. Consistent with the time-reversal invariance of the pairing state, the spin polarization is odd in the surface momentum. Upon bringing the superconductor

into contact with a ferromagnetic insulator, the flatband states therefore acquire a *chiral* dispersion due to the coupling to the exchange field and hence carry a sizable charge current along the interface. The current displays a remarkable singular dependence on the exchange-field strength: Only an infinitesimal exchange field is required to generate a large current, and small changes in the external field can switch the current’s sign. In contrast, doubly degenerate flatbands, when present, give a much weaker contribution to the current. We further show that the interface current for a *fully gapped* NCS is small and not simply related to the presence of spin-polarized edge states.

*Model Hamiltonian.*—Quasiparticle motion in an NCS is described by the Bogoliubov–de Gennes Hamiltonian  $H = \sum_{\mathbf{k}} \Psi_{\mathbf{k}}^{\dagger} H_{\mathbf{k}} \Psi_{\mathbf{k}}$ , with  $\Psi_{\mathbf{k}} = (c_{\mathbf{k}\uparrow}, c_{\mathbf{k}\downarrow}, c_{-\mathbf{k}\uparrow}^{\dagger}, c_{-\mathbf{k}\downarrow}^{\dagger})^T$  and

$$H_{\mathbf{k}} = \begin{pmatrix} \varepsilon_{\mathbf{k}} \sigma_0 - \lambda \mathbf{l}_{\mathbf{k}} \cdot \boldsymbol{\sigma} & (\psi_{\mathbf{k}} \sigma_0 + \mathbf{d}_{\mathbf{k}} \cdot \boldsymbol{\sigma}) i \sigma_y \\ -i \sigma_y (\psi_{\mathbf{k}}^* \sigma_0 + \mathbf{d}_{\mathbf{k}}^* \cdot \boldsymbol{\sigma}) & -\varepsilon_{\mathbf{k}} \sigma_0 - \lambda \mathbf{l}_{\mathbf{k}} \cdot \boldsymbol{\sigma}^* \end{pmatrix}. \quad (1)$$

Here,  $\boldsymbol{\sigma}$  is the vector of Pauli matrices. The normal part of the Hamiltonian describes a two-dimensional square lattice with nearest-neighbor hopping and chemical potential  $\mu$ ,  $\varepsilon_{\mathbf{k}} = 2t(\cos k_x + \cos k_y) - \mu$ , and Rashba SOC with  $\mathbf{l}_{\mathbf{k}} = \hat{x} \sin k_y - \hat{y} \sin k_x$  and strength  $\lambda$ . The even-parity spin-singlet and odd-parity spin-triplet superconducting gaps are written as  $\psi_{\mathbf{k}} = \Delta_0 f(\mathbf{k}) q$  and  $\mathbf{d}_{\mathbf{k}} = \Delta_0 f(\mathbf{k}) \mathbf{l}_{\mathbf{k}} (1 - q)$ , respectively, where the parameter  $q$  tunes between purely spin-triplet ( $q = 0$ ) and purely spin-singlet ( $q = 1$ ) pairings. The structure factor  $f(\mathbf{k})$  fixes the orbital-angular-momentum pairing state. Here, we focus on the nodal ( $d_{xy} + p$ )-wave state [18] described by  $f(\mathbf{k}) = \sin k_x \sin k_y$ . We also present contrasting results for the fully gapped ( $s + p$ )-wave state [23–25] with  $f(\mathbf{k}) = 1$ . In our calculations, we fix  $(t, \mu, \lambda, \Delta_0) = (2.0, 4.0, -2.0, 0.5)$ . Different values of these parameters do not qualitatively change our results.

*Edge states.*—The topological properties of the NCS are best revealed by examining the subgap edge states. To that

end, we compute the spin- and momentum-resolved local density of states (LDOS) of Hamiltonian (1) in a ribbon of width  $L_x$  with edges perpendicular to the (10) direction. The momentum-resolved LDOS and spin LDOS in the  $n$ th layer are given by

$$\rho_n(E, k_y) = -\frac{1}{4\pi} \text{Im}[\text{Tr}\{G_{k_y}(n, n; E)\}], \quad (2a)$$

$$\rho_n^\mu(E, k_y) = -\frac{\hbar}{4\pi} \text{Im}[\text{Tr}\{\check{S}^\mu G_{k_y}(n, n; E)\}], \quad (2b)$$

respectively, where  $\check{S}^\mu = \text{diag}(\sigma^\mu, -[\sigma^\mu]^*)$ , and  $G_{k_y}(n, n'; E) = -i \int_{-\infty}^{\infty} dt e^{iEt} \langle T_t \Psi_{nk_y}(t) \Psi_{n'k_y}^\dagger(0) \rangle$  is the zero-temperature Green's function with  $\Psi_{nk_y} = (2\pi L_x)^{-1/2} \sum_{\mathbf{k}} \Psi_{\mathbf{k}} e^{-ik_x n}$ . The expressions in Eqs. (2) are evaluated for ribbons of width up to  $L_x = 10^3$  and an intrinsic broadening  $\eta = 0.005$ . Figure 1 shows the LDOS integrated over the ten outermost layers, which is on the order of the localization length of the subgap state. Both subgap edge states [gray (dark red)] and continuum bulk states [light gray (orange and yellow)] are visible.

The nodal character of the  $(d_{xy} + p)$ -wave state precludes the existence of a global topological number. By treating every point in the edge Brillouin zone as the edge of a one-dimensional system, however, one can define a momentum-dependent winding number  $W_{(10)}(k_y)$ , which only changes across projected nodes of the bulk gap [7,8,19,21]. In particular, one finds  $W_{(10)}(k_y) = \pm 1$  for  $k_y$  lying between the projected edges  $k_{F,+}$  and  $k_{F,-}$  of the two spin-orbit-split Fermi surfaces, i.e.,  $|k_y| \in [k_{F,+}, k_{F,-}] \simeq [0.352\pi, 0.648\pi]$ . This ensures the existence of nondegenerate zero-energy flatbands at these momenta  $k_y$ , which are clearly visible in Figs. 1(a) and 1(c). For  $|k_y| < k_{F,+}$ , on the other hand, there are topologically trivial dispersing states for dominant triplet pairing, and doubly degenerate zero-energy flatbands with  $W_{(10)}(k_y) = \pm 2$  when singlet pairing dominates. In contrast, for  $q < q_{c,L} \simeq 0.472$  and  $q > q_{c,U} \simeq 0.583$ , the  $(s + p)$ -wave NCS is a fully gapped superconductor in symmetry class DIII. For  $q < q_{c,L}$ , the superconductor has a topologically nontrivial character with a nonzero  $\mathbb{Z}_2$  topological number [2,25,26], and by the bulk-boundary correspondence there are helical Majorana subgap states; see Fig. 1(e) [23–25]. For  $q > q_{c,U}$ , the system is topologically trivial and there are no edge states [Fig. 1(g)].

Similarly to other topological systems with strong SOC [1,27], the NCS edge states exhibit a distinct spin texture. It is well known that the electronlike part of the edge-state wave function is strongly spin polarized [24]. The total spin polarization, which includes both electronlike and holelike polarizations, is also nonvanishing. Importantly, the exchange field couples to the total spin polarization, not just to the electronlike contribution. In both NCS models, we find that the continuum and subgap states show a strong total polarization in the  $xz$ -spin plane but a vanishing

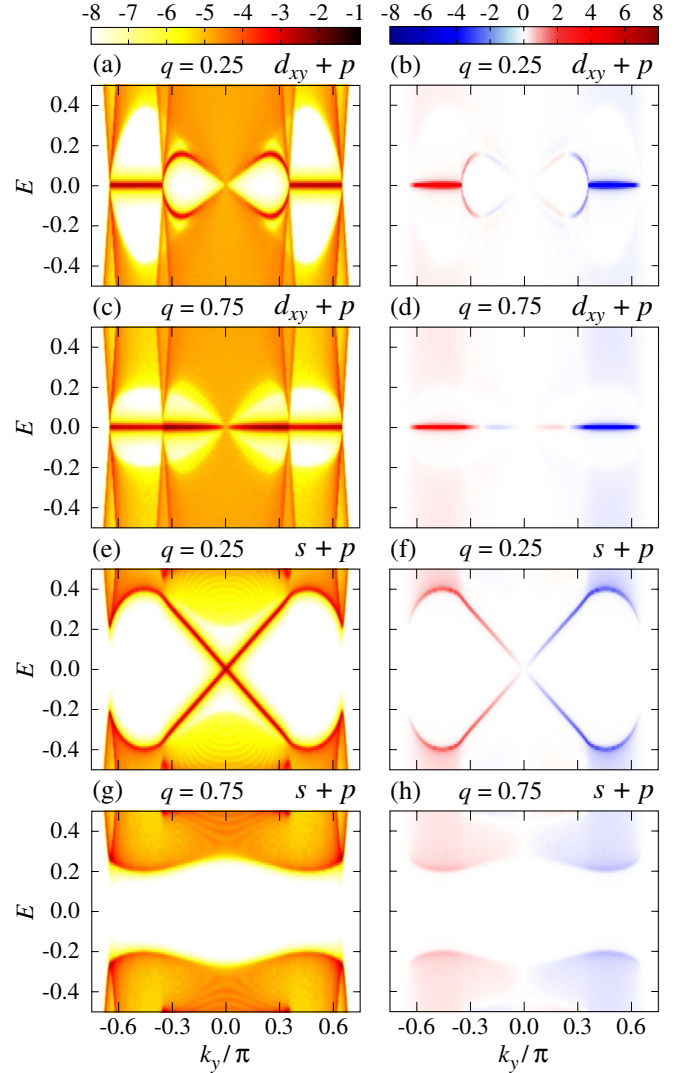


FIG. 1 (color online). Left column: Momentum-resolved LDOS on a log scale for the ten outermost layers at the (10) edge of the  $(d_{xy} + p)$ -wave NCS with (a)  $q = 0.25$  and (c)  $q = 0.75$ , and for the  $(s + p)$ -wave NCS with (e)  $q = 0.25$  and (g)  $q = 0.75$ . In the right column, we present the corresponding  $x$  component of the momentum-resolved spin LDOS for the outermost layer in units of  $\hbar/20$  on a linear scale. The  $z$  component of the momentum-resolved spin LDOS is provided in Fig. S1 of the SM [29].

$y$  component [28]. We present the  $x$ -spin polarization in the right-hand column of Fig. 1 and the  $z$ -spin polarization in Fig. S1 of the Supplemental Material (SM) [29]. The magnitude and sign of the polarization are strongly momentum dependent and display a complicated interplay between the singlet-triplet ratio  $q$  and the SOC strength  $\lambda$ . The nondegenerate zero-energy flatbands of the  $(d_{xy} + p)$ -wave NCS exhibit a particularly strong and robust  $x$ -spin polarization, whereas the  $z$ -spin polarization is smaller and changes sign close to  $\pm(k_{F,-} - k_{F,+})/2$  [29]. This is in contrast to the doubly degenerate states in

the singlet-dominated state, which give opposite contributions to the spin LDOS of unequal magnitude, overall leading to a weaker spin polarization than for the non-degenerate states. As required by time-reversal symmetry, subgap states with opposite edge momenta have opposite spin polarizations. This enhances the robustness of the nondegenerate flatbands, as time-reversal-invariant scattering processes connecting the oppositely  $x$ -spin-polarized states at  $+k_y$  and  $-k_y$  are strongly suppressed.

The nontrivial spin character of the edge states could be inferred from the absence of large- $k_y$  backscattering processes in quasiparticle interference measurements. Another possibility is to study the response of the subgap states upon bringing the NCS into contact with a ferromagnetic insulator. We anticipate that the proximity-induced exchange field  $\mathbf{H}_{\text{ex}}$  will lead to a perturbative correction to the energy of the spin-polarized edge states proportional to  $\sum_{\mu=1}^3 H_{\text{ex}}^{\mu} \rho_1^{\mu}(E, k_y)$ . Since the flatband states at  $+k_y$  and  $-k_y$  are oppositely spin polarized, the coupling to the exchange field will shift the energy of these edge states in opposite directions, hence converting them into *chirally* dispersing modes. Similarly, the left- and right-moving helical edge states of the  $(s+p)$ -wave NCS should acquire different velocities. To test this, we show in Fig. 2 the momentum-resolved LDOS when an exchange field  $\mathbf{H}_{\text{ex}} = 0.4\hat{x}$  is applied to the leading edge. Here and in the rest of this Letter, we will specialize to an  $x$ -oriented exchange field; results for a field along the  $z$  axis are included in the SM [29]. Comparison with Fig. 1 reveals that the edge states of both NCS systems indeed display a linear shift in

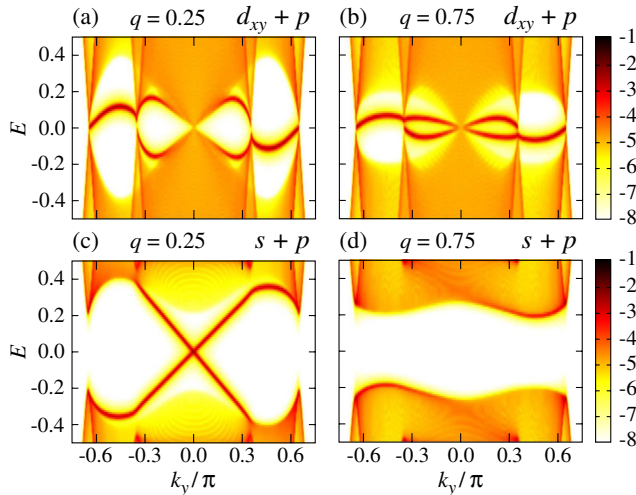


FIG. 2 (color online). Momentum-resolved LDOS at the (10) edge of (a),(b) the  $(d_{xy} + p)$ -wave and (c),(d) the  $(s + p)$ -wave NCSs in the presence of an exchange field along the  $x$  axis with  $H_{\text{ex}}^x = 0.4$ , applied to the edge layer  $n = 1$ . In the left column, we have  $q = 0.25$  (majority triplet), while in the right column, we plot results for  $q = 0.75$  (majority singlet). As in Fig. 1, we use a log color scale.

energy, which is to a good approximation proportional to  $H_{\text{ex}}^x \rho_1^x(E, k_y)$ , as long as  $|H_{\text{ex}}^x| \lesssim \Delta_0$ .

*Edge currents.*—The chiral structure of the edge states induced by the exchange field naturally suggests the presence of a spontaneous edge current in the NCS. In particular, the chiral mode originating from the flatbands can be expected to carry a current comparable to that in a chiral  $p$ -wave superconductor. The zero-temperature expectation value of the surface component of the current is written in terms of the momentum-resolved LDOS and spin LDOS as

$$I_y = \frac{e}{2\hbar} \frac{1}{N_y} \sum_{k_y} \sum_{n=1}^{L_x/2} \int_{-\infty}^0 dE \{ 2t \sin k_y \rho_n(E, k_y) - \lambda \cos k_y \rho_n^x(E, k_y) \}. \quad (3)$$

Here,  $N_y$  is the number of  $k_y$  points in the edge Brillouin zone. The first term in the braces is the contribution from nearest-neighbor hopping, whereas the second term is due to the SOC.

In Fig. 3, we plot the edge current  $I_y$  as a function of singlet-triplet parameter  $q$  and exchange field along the  $x$  axis. We indeed find spontaneous currents flowing along the edge of the NCS for both gap symmetries, but the two cases are dramatically different. In particular, the current in the  $(d_{xy} + p)$ -wave NCS exhibits striking deviations from linear response behavior: As seen in Fig. 3(a), an infinitesimally small exchange field is sufficient to generate a

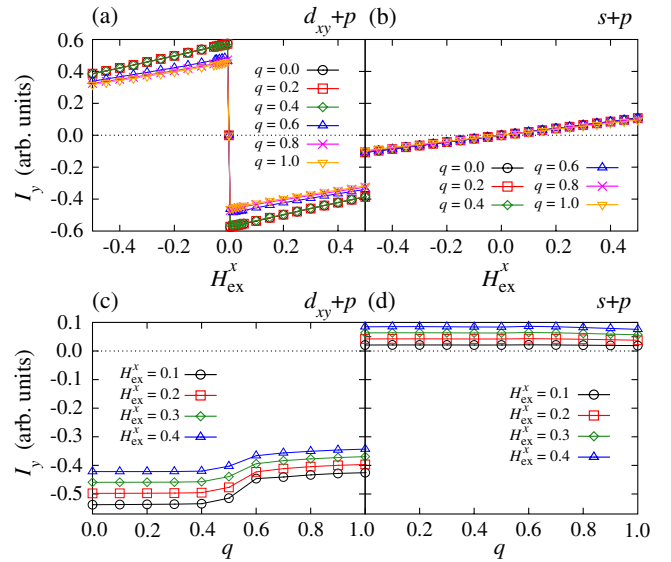


FIG. 3 (color online). Top row: Zero-temperature edge current  $I_y$  as a function of the exchange field  $H_{\text{ex}}^x$  for various values of the singlet-triplet parameter  $q$  for (a) the  $(d_{xy} + p)$ -wave and (b) the  $(s + p)$ -wave NCSs. Bottom row:  $I_y$  as a function of the singlet-triplet parameter  $q$  for various exchange fields along the  $x$  axis, applied to the leading edge of (c) the  $(d_{xy} + p)$ -wave and (d) the  $(s + p)$ -wave NCSs. For comparison, the edge current of a chiral  $p$ -wave superconductor without an exchange field and SOC is about 0.64 in our units.

large current in the NCS, and the current abruptly switches sign as the exchange field is reversed. Remarkably, the magnitude of the current *decreases* with increasing exchange field from a maximum magnitude at  $H_{\text{ex}}^x \rightarrow \pm 0$ , which is about 90% of the one for a chiral  $p$ -wave superconductor with vanishing SOC. Although the current is somewhat larger for triplet-dominated pairing, it depends only weakly on  $q$  away from the singlet-triplet crossover ( $q_{c,L} < q < q_{c,U}$ ), as shown in Fig. 3(c). In contrast, the current in the  $(s + p)$ -wave NCS is always much smaller and grows linearly with the exchange field; see Figs. 3(b) and 3(d). Unexpectedly, there is almost no dependence upon the singlet-triplet parameter  $q$ , despite the qualitative change of the subgap spectrum with the topological transition at  $q = q_{c,L}$ .

To gain a better understanding of the origin of the currents, it is instructive to examine the current  $I_y(k_y)$  contributed by states at  $+k_y$  and  $-k_y$ , i.e., the even part of the  $k_y$  summand in Eq. (3). In Fig. 4, we show the evolution of  $I_y(k_y)$  with the singlet-triplet parameter  $q$  for an exchange field along the  $x$  axis. The current in the  $(d_{xy} + p)$ -wave NCS is dominated by the contribution from states with  $k_{F,+} < |k_y| < k_{F,-}$ , i.e., the momenta at which we find the chiral mode originating from the nondegenerate flatbands. The current displays no variation with  $q$  in this momentum range and is almost independent of the exchange-field strength (not shown) and hence accounts for most of the singular response seen in Fig. 3(a). The linear decrease of the total current with increasing exchange field originates from the contribution at  $|k_y| < k_{F,+}$ . Intriguingly, in this region, there is also a small singular response in the singlet-dominated regime, accounting for the reduced jump in the total current in Fig. 3(a). Its origin will be discussed briefly below. The profile of  $I_y(k_y)$  in the  $(s + p)$ -wave NCS shows that the edge current is in this case due to states with  $|k_y| < k_{F,+}$ . Although this is the momentum range in which the helical

edge states are realized for  $q < q_{c,L}$ , there is little  $q$  dependence of the momentum-resolved currents. We hence conclude that the current is largely insensitive to the helical edge states.

*Discussion.*—The strong edge current in the  $(d_{xy} + p)$ -wave NCS is primarily carried by the chiral edge mode originating from the nondegenerate flatbands. Although the exchange field induces chiral structures in all the edge states, only this mode is *uncompensated* by a counter-propagating state. For example, even though they have different velocities, the left- and right-moving edge states in the  $(s + p)$ -wave NCS still carry identical currents in opposite directions at zero temperature. This statement can be formalized by examining Eq. (3): Only the hopping term is sensitive to the chiral structure, as it is proportional to the difference between the number of states (integrated LDOS) below the Fermi energy at  $+k_y$  and  $-k_y$ . Inspection of Fig. 2 clearly shows that only the opposite energy shift of the oppositely polarized nondegenerate flatbands can generate such a number difference. The singular behavior of the current immediately follows, as the number difference appears even for infinitesimal field strength, and does not change as the field is increased. The hopping contribution is vanishing in all other cases, and the current is instead due to the SOC term in Eq. (3), which is proportional to the sum of the  $x$ -spin polarization at  $+k_y$  and  $-k_y$ . This naturally connects the linear variation of the current with field strength to the induced surface magnetization.

In the case of the majority-singlet  $(d_{xy} + p)$ -wave NCS, however, the splitting of the doubly degenerate flatbands for  $|k_y| < k_{F,+}$  also gives a small singular response to the exchange field, as even an infinitesimal shift of the negatively (positively) spin-polarized states below (above) the Fermi energy generates a finite  $x$ -spin polarization. The current from the doubly degenerate states nevertheless increases monotonically with exchange-field strength, and so the overall decreasing current remains a signature of the nondegenerate flatbands. The doubly degenerate flatbands are also distinguished by their dependence on the exchange-field orientation. While the magnitude of the current contributed by the doubly degenerate flatbands is equal for both  $x$ - and  $z$ -oriented fields, the current due to the nondegenerate flatbands undergoes a large change as the field is rotated from the  $x$  to the  $z$  axis [29].

Although we have specified our discussion to the case of an insulating ferromagnet, we note that an edge current is also induced by placing the NCS in contact with a ferromagnetic *metal* [30,31]. The observation of a large edge current at the interface between an NCS and any ferromagnet would therefore be strong proof of the existence of nondegenerate flatbands. Experimental detection of the edge currents should be possible in spite of the Meissner effect, which implies that screening currents exactly compensate the edge currents in a large sample. However,

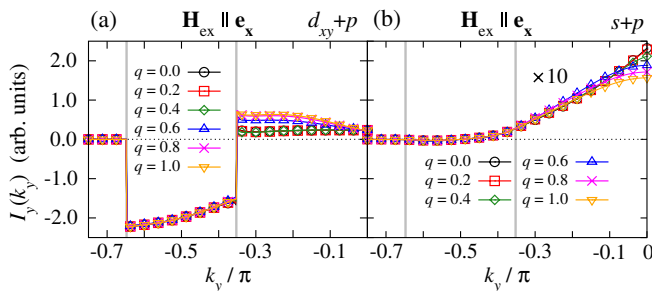


FIG. 4 (color online). Momentum-resolved edge current  $I_y(k_y)$  for various values of singlet-triplet parameter  $q$  in (a) the  $(d_{xy} + p)$ -wave and (b) the  $(s + p)$ -wave NCSs. The exchange field is  $H_{\text{ex}}^x = 0.2$ . The vertical gray lines indicate the projections of the edges of the two spin-orbit-split Fermi surfaces  $|k_y| = k_{F,\pm}$ . Note that the  $(s + p)$ -wave results are multiplied by 10 for clarity.

whereas the edge-current density decays into the bulk on the scale of the coherence length  $\xi_0$ , the screening only builds up over the scale of the penetration depth  $\lambda_L$ . For an extreme type-II superconductor, characteristic of many NCSs [11], the screening currents will therefore be suppressed in a sample of width  $W$  with  $\xi_0 \ll W \ll \lambda_L$ . This argument also holds for an engineered NCS [32].

*Summary.*—We have proposed a novel test of nondegenerate flatbands at the edge of a topological NCS based on their response to an exchange field. Specifically, we have shown that due to their strong spin polarization, they acquire a chiral dispersion when placed in contact with a ferromagnet. The resulting current shows a characteristic singular dependence upon the exchange-field strength and dominates the current due to other edge states, including doubly degenerate flatbands.

The authors thank M. Sigrist for useful discussions. A. P. S. thanks NORDITA for its hospitality and financial support. C. T. acknowledges financial support by the Deutsche Forschungsgemeinschaft through Research Training Group GRK 1621.

\*a.schnyder@fkf.mpg.de

†carsten.timm@tu-dresden.de

‡brydon@theory.phy.tu-dresden.de

- [1] M. Hasan and C. Kane, *Rev. Mod. Phys.* **82**, 3045 (2010).
- [2] S. Ryu, A. P. Schnyder, A. Furusaki, and A. W. W. Ludwig, *New J. Phys.* **12**, 065010 (2010).
- [3] X.-L. Qi and S.-C. Zhang, *Rev. Mod. Phys.* **83**, 1057 (2011).
- [4] A. P. Schnyder, S. Ryu, A. Furusaki, and A. W. W. Ludwig, *Phys. Rev. B* **78**, 195125 (2008).
- [5] A. M. Turner and A. Vishwanath, [arXiv:1301.0330](https://arxiv.org/abs/1301.0330).
- [6] X. Wan, A. M. Turner, A. Vishwanath, and S. Y. Savrasov, *Phys. Rev. B* **83**, 205101 (2011).
- [7] A. P. Schnyder and S. Ryu, *Phys. Rev. B* **84**, 060504(R) (2011).
- [8] Y. Tanaka, M. Sato, and N. Nagaosa, *J. Phys. Soc. Jpn.* **81**, 011013 (2012).
- [9] Y. X. Zhao and Z. D. Wang, *Phys. Rev. Lett.* **110**, 240404 (2013).
- [10] S. Matsuura, P.-Y. Chang, A. P. Schnyder, and S. Ryu, *New J. Phys.* **15**, 065001 (2013).
- [11] *Non-Centrosymmetric Superconductors: Introduction and Overview*, edited by E. Bauer and M. Sigrist, Lecture Notes in Physics Vol. 847 (Springer, Berlin, 2012).
- [12] K. Izawa, Y. Kasahara, Y. Matsuda, K. Behnia, T. Yasuda, R. Settai, and Y. Onuki, *Phys. Rev. Lett.* **94**, 197002 (2005).
- [13] I. Bonalde, R. L. Robeiro, W. Brämer-Escamilla, C. Rojas, E. Bauer, A. Prokofiev, Y. Haga, T. Yasuda, and Y. Onuki, *New J. Phys.* **11**, 055054 (2009).
- [14] H. Mukuda, T. Fujii, T. Ohara, A. Harada, M. Yashima, Y. Kitaoka, Y. Okuda, R. Settai, and Y. Onuki, *Phys. Rev. Lett.* **100**, 107003 (2008).
- [15] H. Q. Yuan, D. F. Agterberg, N. Hayashi, P. Badica, D. Vandervelde, K. Togano, M. Sigrist, and M. B. Salamon, *Phys. Rev. Lett.* **97**, 017006 (2006).
- [16] M. Nishiyama, Y. Inada, and G.-Q. Zheng, *Phys. Rev. Lett.* **98**, 047002 (2007).
- [17] G. Eguchi, D. C. Peets, M. Kriener, S. Yonezawa, G. Bao, S. Harada, Y. Inada, G.-q. Zheng, and Y. Maeno, *Phys. Rev. B* **87**, 161203(R) (2013).
- [18] Y. Tanaka, Y. Mizuno, T. Yokoyama, K. Yada, and M. Sato, *Phys. Rev. Lett.* **105**, 097002 (2010).
- [19] M. Sato, Y. Tanaka, K. Yada, and T. Yokoyama, *Phys. Rev. B* **83**, 224511 (2011); K. Yada, M. Sato, Y. Tanaka, and T. Yokoyama, *Phys. Rev. B* **83**, 064505 (2011).
- [20] P. M. R. Brydon, A. P. Schnyder, and C. Timm, *Phys. Rev. B* **84**, 020501(R) (2011).
- [21] A. P. Schnyder, P. M. R. Brydon, and C. Timm, *Phys. Rev. B* **85**, 024522 (2012).
- [22] J. P. Dahlhaus, M. Gibertini, and C. W. J. Beenakker, *Phys. Rev. B* **86**, 174520 (2012).
- [23] C. Iniotakis, N. Hayashi, Y. Sawa, T. Yokoyama, U. May, Y. Tanaka, and M. Sigrist, *Phys. Rev. B* **76**, 012501 (2007).
- [24] A. B. Vorontsov, I. Vekhter, and M. Eschrig, *Phys. Rev. Lett.* **101**, 127003 (2008); Y. Tanaka, T. Yokoyama, A. V. Balatsky, and N. Nagaosa, *Phys. Rev. B* **79**, 060505(R) (2009); C.-K. Lu and S.-K. Yip, *Phys. Rev. B* **82**, 104501 (2010).
- [25] M. Sato and S. Fujimoto, *Phys. Rev. B* **79**, 094504 (2009).
- [26] X.-L. Qi, T. L. Hughes, S. Raghu, and S.-C. Zhang, *Phys. Rev. Lett.* **102**, 187001 (2009).
- [27] D. Sticlet, C. Bena, and P. Simon, *Phys. Rev. Lett.* **108**, 096802 (2012).
- [28] The doubly degenerate zero-energy states in both NCS models have equal and opposite  $y$ -spin polarization. Thus, although  $\rho_n^y(E, k_y)$  is always vanishing, these states are split by an exchange field along the  $y$  axis [19,25].
- [29] See Supplemental Material at <http://link.aps.org/supplemental/10.1103/PhysRevLett.111.077001> for the  $z$  component of the spin LDOS and the effect of an exchange field along the  $z$  axis.
- [30] P. M. R. Brydon, C. Timm, and A. P. Schnyder, *New J. Phys.* **15**, 045019 (2013).
- [31] C.-D. Ren and J. Wang, *Eur. Phys. J. B* **86**, 190 (2013).
- [32] S. Takei, B. M. Fregoso, V. Galitski, and S. Das Sarma, *Phys. Rev. B* **87**, 014504 (2013); F. Zhang, C. L. Kane, and E. J. Mele, *Phys. Rev. Lett.* **111**, 056402 (2013).